

First principles calculation to investigate the structural, electronic, elastic, mechanical, and optical properties of K_2NiP_2 ternary compound

Cite as: AIP Advances **12**, 105018 (2022); <https://doi.org/10.1063/5.0118809>

Submitted: 06 August 2022 • Accepted: 03 October 2022 • Published Online: 28 October 2022

 Mwende Mbilo and  Robinson Musembi



View Online



Export Citation



CrossMark

ARTICLES YOU MAY BE INTERESTED IN

[Features of gate-tunable and photon-field-controlled optoelectronic processes in a molecular junction: Application to a ZnPc-based transistor](#)

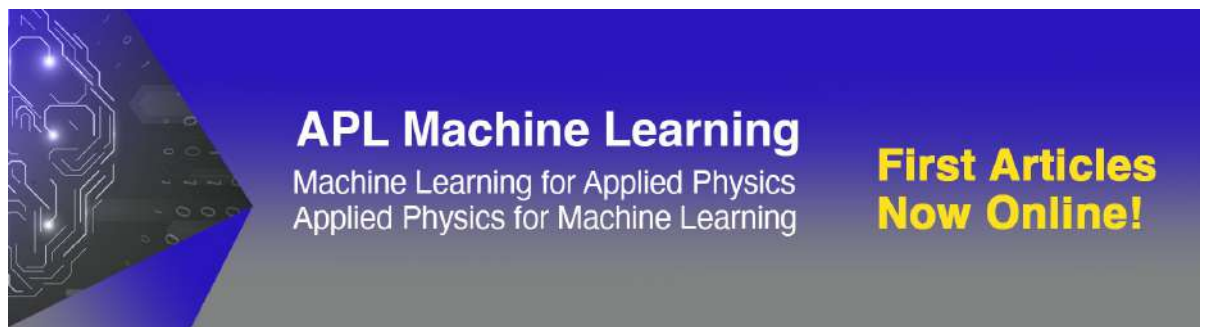
AIP Advances **12**, 105020 (2022); <https://doi.org/10.1063/5.0119257>

[A Bayesian data assimilation method to enhance the time sequence prediction ability of data-driven models](#)

AIP Advances **12**, 105021 (2022); <https://doi.org/10.1063/5.0119688>

[Influence of high pressure pulsating excitation on pipe joint sealing based on multiscale contact analyses](#)

AIP Advances **12**, 105022 (2022); <https://doi.org/10.1063/5.0104671>



APL Machine Learning
Machine Learning for Applied Physics
Applied Physics for Machine Learning

**First Articles
Now Online!**

First principles calculation to investigate the structural, electronic, elastic, mechanical, and optical properties of K_2NiP_2 ternary compound

Cite as: AIP Advances 12, 105018 (2022); doi: 10.1063/5.0118809

Submitted: 6 August 2022 • Accepted: 3 October 2022 •

Published Online: 28 October 2022



View Online



Export Citation



CrossMark

Mwende Mbilo  and Robinson Musembi^{a)} 

AFFILIATIONS

Department of Physics, Faculty of Science and Technology, University of Nairobi, P.O. Box 30197–00100, Nairobi, Kenya

^{a)} Author to whom correspondence should be addressed: musembirj@uonbi.ac.ke

ABSTRACT

First-principles calculations of the structural, electronic, elastic, mechanical, and optical properties of the K_2NiP_2 ternary compound using density functional theory as implemented in the quantum espresso package have been performed. The calculations have been done using the generalized gradient approximation (GGA) with the Perdew–Burke–Ernzerhof (PBE, PBEsol) exchange-correlation functionals and the local density approximation (LDA). The lattice parameters have been found to agree with the available experimental results. Direct bandgaps have been obtained as 0.630, 0.588, and 0.525 eV when using the GGA-PBE, GGA-PBEsol, and LDA approximations, respectively. In all three scenarios, the valence bands have been noted to be majorly formed by Ni-3d and P-2p states with little contribution from the other states, whereas the conduction bands have been observed to be mainly formed by P-2p states with a small contribution from the other states. The K_2NiP_2 has been found to be mechanically stable, ductile, and ionic. The optical properties showed that the compound under investigation has a high refractive index and absorption coefficients covering the ultraviolet–visible regions, thus indicating its potential for photovoltaic applications. The bandgaps obtained using LDA were smaller than those obtained using GGA. This is because LDA underestimates the bandgaps.

© 2022 Author(s). All article content, except where otherwise noted, is licensed under a Creative Commons Attribution (CC BY) license (<http://creativecommons.org/licenses/by/4.0/>). <https://doi.org/10.1063/5.0118809>

I. INTRODUCTION

Since the beginning of the industrial age to the present today, semiconductor materials have played an important role in making them some of the most sought-after materials for the last few decades due to their potential in optoelectronics applications. The first generation of these materials were unary semiconductors from Periodic Table groups IV_A and VI_A , mainly consisting of silicon (Si), germanium (Ge), selenium (Se), and tellurium (Te).^{1–3} Further combinations to form binary semiconductors, apart from forming new compound semiconductors, had a tremendous effect on the properties of the new materials, such as optical, electrical, structural, and mechanical properties. Examples of such second generation compound semiconductors are GaAs and CdTe. Improvement in technology and synthesis techniques further enabled the

formation of more complex combinations like the ternary and quaternary semiconductors with more superior properties that can be engineered for a specific application or fine-tuned to suit different flavors of the electromagnetic spectrum.^{4–8}

A number of half metallic and semiconductor ABC types of ternary compounds exist with different types of applications, such as Heusler alloys, Kesterite, Chalcogenides, and Perovskites. Over the past decades, ternary semiconductor compounds with the ABC_2 -type crystal structure have been extensively investigated owing to their good electronic and optical properties suitable for a variety of optoelectronic and photovoltaic applications.^{9–12} The ABC_2 -type ternary compounds are classified into chalcogenides ($A^I B^{III} C_2^{VI}$) and pnictides ($A^{II} B^{IV} C_2^V$),¹⁰ both of which are made up of inorganic, non-toxic, and abundant earth elements. These ABC_2 -type materials have shown good potential as alternatives

to the expensive and toxic crystalline Silicon, amorphous Silicon, copper indium gallium selenide, and cadmium Telluride, among others, which are currently dominating the optoelectronic and photovoltaic industries.¹³ However, the full realization of the potential of these ABC₂-type compounds for diverse technological applications is not yet achieved. Therefore, researchers are constantly pursuing further studies on the properties of these materials.

Recently, Lathwal *et al.*¹⁴ investigated the BeSnN₂ ternary compound for optoelectronic applications using the density functional theory (DFT) approach. Yaseen *et al.*¹⁵ studied the electronic, transport, and optical properties of NaGaX₂ (X = S, Se, Te) compounds using DFT for photovoltaic applications. The optoelectronic and thermoelectric properties of ACuS₂ (A = Al, Ga, In) have been investigated¹⁶ for potential optoelectronic, thermoelectric, and photovoltaic applications using a combined Boltzmann transport theory and DFT. In a recent approximation using the DFT approach,¹⁷ CuTiX₂ (X = S, Se, and Te) has been found to exhibit good electronic properties suitable for solar cell applications. Additionally, AlGaX₂ (X = As, Sb) compounds have been found suitable for optoelectronic and thermoelectric device applications by using first-principles calculations based on DFT. Further studies on the ABC₂-type ternary compounds for various technological applications have been reported.^{18–25}

The ABC₂-type ternary compounds (A = I_A, B = VIII, C = V_A) based on potassium elements have been less studied. Specifically, the ternary compounds with the K–Ni–P compositions have been less reported in the literature apart from a few exceptions.^{26,27} To the best of our knowledge, there is only a single experimental report in the literature on the crystal structure design of the K₂NiP₂ ternary compound,²⁷ hence the motivation for this investigation. To fully realize the potential of the K₂NiP₂ ternary compound for possible technological applications, a theoretical investigation is essential. For this reason, we have investigated the structural, electronic, elastic, mechanical, and optical properties of the K₂NiP₂ ternary compound using the generalized gradient approximation (GGA) and the local density approximation (LDA) based on density functional theory.

II. COMPUTATIONAL METHODS

All the computations were performed using first principle methods based on DFT.^{28,29} The calculations were executed using the projector augmented wave (PAW) potentials³⁰ using the quantum espresso code.³¹ The electron–ion interaction^{32,33} was treated within the generalized gradient approximation, using PBE, PBEsol, and LDA as the exchange correlation functional.^{34,35} The local density approximation and the generalized gradient approximation pseudopotentials are related mathematically as follows: the local density approximation is given as

$$E_{xc}^{LDA} = \int d\vec{r} n(\vec{r}) \varepsilon_{xc}^{hom}(n(\vec{r})), \quad (1)$$

where $\varepsilon_{xc}^{hom}(n(\vec{r}))$ is the homogeneous exchange correlation energy density of the electron gas, while the generalized gradient approximation is given as

$$E_{xc}^{GGA} = \int d\vec{r} f n(\vec{r}) \cdot \nabla n(\vec{r}), \quad (2)$$

where $\nabla n(\vec{r})$ are the gradients, whereby there are different flavors of GGA, each of which takes a different $f n(\vec{r})$ function.^{33,36–38}

The K₂NiP₂ crystal structure input file was downloaded from the materials project,^{39–41} and the materials cloud input file generator implemented in quantum espresso (QE) was used to generate the Plane Wave self-consistent field (PWscf) input file as well as the pseudopotentials⁴² for DFT calculations. We use a plane-wave basis set with a kinetic energy cutoff of 150 Ry and a Monkhorst–Pack k-point grid of 9 × 9 × 9 with an offset of 1. Geometry optimization is performed by computing the total energy per unit cell at various lattice constant values to obtain the ground state structural properties. The optimized lattice parameters thus obtained are used for further computations of electronic, elastic, mechanical, and optical properties.

III. RESULTS AND DISCUSSION

A. Structural properties

The K₂NiP₂ crystallizes in the orthorhombic three-dimensional crystal structure²⁷ as shown in Fig. 1.

The computed K–P bond distance was found to be shorter than the K–Ni bond distance as presented in Table I. The values computed for the bond distances within the K₂NiP₂ crystal lattice parameters are slightly different from those given in the experimental results,²⁷ and this is attributed to the fact that the cell volume used in this work was 249.111 Å³, while the volume in the literature was 495.3 Å³. The geometry optimization was done by minimizing the total energy as a function of the unit cell lattice constants as illustrated in Figs. 2(a)–2(c).

After geometry optimization, the total energy and lattice constant values were fitted in the Birch–Murnaghan equation of state⁴³ to obtain the ground-state lattice parameters. The obtained ground-state lattice parameters as presented in Table II are consistent with the ones reported elsewhere.²⁷

B. Electronic properties

The electronic properties,^{44,45} including band structure and projected density of states (PDOS), describe the bandgap, the direct/indirect nature of the bandgap, the location of the Fermi level,

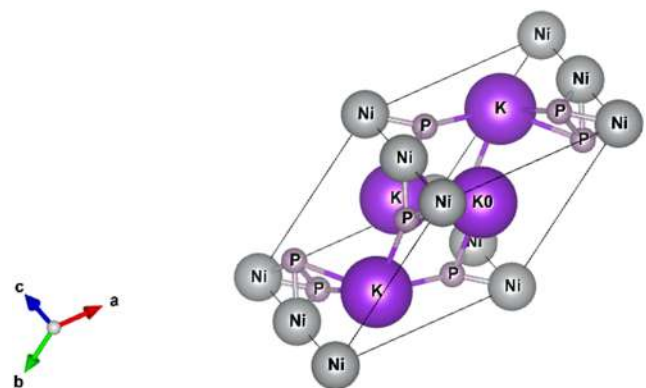


FIG. 1. Crystal structure of orthorhombic K₂NiP₂ ternary compound.

TABLE I. Bond lengths within the K_2NiP_2 crystal structure.

Bond	Bond distance (Å)
K–Ni	3.2639
Ni–P	2.2553

the density of states, as well as the atomic and orbital contributions to the formation of the valence and conduction bands. The occurrence of the valence band maxima and conduction band minima at two similar/different symmetry points in the first Brillouin zone symbolizes the direct/indirect nature of the bandgap.^{46,47} In this work, the direct bandgaps of the K_2NiP_2 semiconductor ternary compound were obtained as 0.630, 0.588, and 0.525 eV, as shown in Figs. 3–5, using the GGA-PBE, GGA-PBEsol, and LDA approximations, respectively. The bandgap obtained using LDA is smaller than the bandgaps obtained using GGA approximations. This is because the application of LDA is known to underestimate semiconductor bandgaps.⁴⁸

The contribution to the formation of the valence bands in all the three approximations in the energy regions -3 eV to the Fermi level was majorly by Ni-3d and P-2p states with little contribution from the other states, whereas the contribution to the formation of the conduction bands was majorly by P-2p states with a small contribution from the other states.

C. Elastic and mechanical properties

K_2NiP_2 ternary compound crystallizes in the orthorhombic (Laue class mmm) crystal structure featuring nine independent elastic constants,⁴⁹ which include C_{11} , C_{12} , C_{13} , C_{22} , C_{23} , C_{33} , C_{44} , C_{55} , and C_{66} . The necessary and sufficient conditions for elastic stability of the orthorhombic crystal structure⁴⁹ are given as

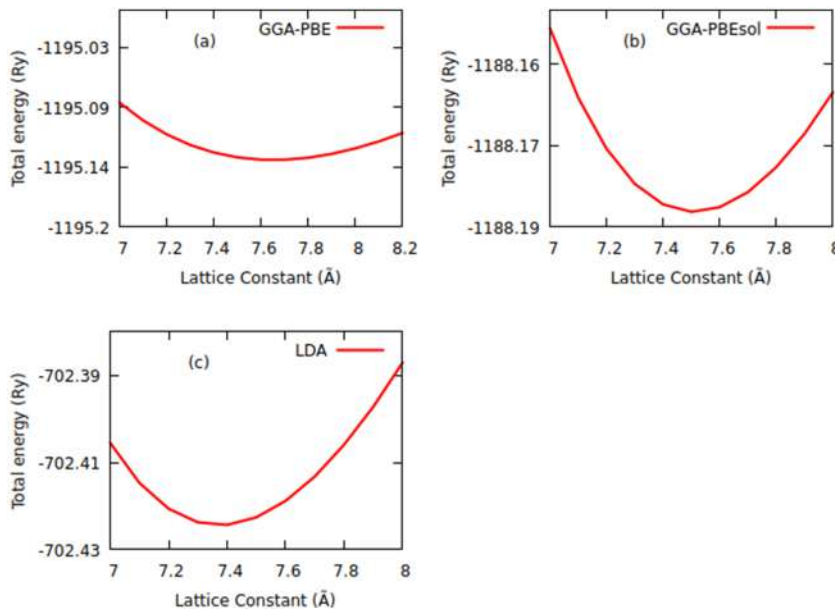
TABLE II. Structural properties of K_2NiP_2 ternary compound.

Properties	GGA-PBE	GGA-PBEsol	LDA
Lattice parameter a_0 (Å)	7.657 34	7.510 50	7.372 71
Lattice parameter b/a	1.790 6	1.790 6	1.790 6
Lattice parameter c/a	0.740 3	0.740 3	0.740 3

$$\begin{cases} C_{11} > 0; C_{11}C_{22} > C_{12}^2, \\ C_{11}C_{22}C_{33} + 2C_{12}C_{13}C_{23} \\ -C_{11}C_{23}^2 - C_{22}C_{13}^2 - C_{33}C_{12}^2 > 0, \\ C_{44} > 0; C_{55} > 0; C_{66} > 0. \end{cases} \quad (3)$$

The computed values of the elastic constants in Table III satisfy the conditions in Eq. (1); hence, the K_2NiP_2 ternary compound is mechanically stable.

Bulk modulus is a measure of resistance against volume change as a result of applied external pressure.⁴⁶ Shear modulus measures incompressibility,⁵⁰ while Young's modulus measures the stiffness of a material.⁵¹ Large B, G, and E predict stronger incompressibility and stiffness of materials. As presented in Table IV, K_2NiP_2 is less stiff and not hard to compress. The ductile/brittle nature of materials is determined by Pugh's ratio B/G .⁵² The restriction for brittleness is $B/G < 1.75$; else, the material is said to be ductile. The Poisson's ratio $\nu = 0.1, 0.25,$ and 0.33 for pure covalent, ionic, and metallic bonds, respectively.⁵³ Therefore, we can conclude that the K_2NiP_2 ternary compound affirms a ductile character using GGA-PBE and a brittle character using (GGA-PBEsol and LDA) approximations. Also, the compound under study is strongly dominated by the ionic character. To the best of our understanding, there are no other studies on the elastic and mechanical properties of the K_2NiP_2 ternary compound to compare our findings with.

**FIG. 2.** Variation of total energy vs lattice constants of K_2NiP_2 ternary compound using the (a) GGA-PBE, (b) GGA-PBEsol, and (c) LDA approximations.

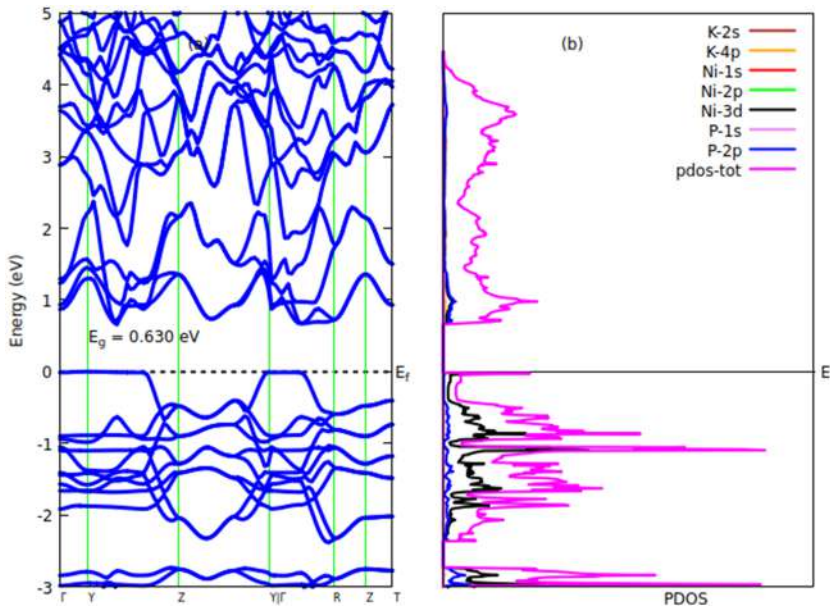


FIG. 3. Calculated (a) band structure and (b) projected density of states of K_2NiP_2 ternary compound using the GGA-PBE approximation.

D. Optical properties

It is needful to investigate the frequency response of various optical parameters to the incident photon radiation to assess the prospect of the K_2NiP_2 ternary compound for photovoltaic applications. The response of electrons in a material is characterized by the complex dielectric wave function,^{54,55} which is described as

$$\varepsilon(\omega) = \varepsilon_1(\omega) + i\varepsilon_2(\omega). \quad (4)$$

In this case, $\varepsilon_1(\omega)$ and $\varepsilon_2(\omega)$ denote the real and imaginary parts of the complex dielectric wave function. From the $\varepsilon_1(\omega)$ and $\varepsilon_2(\omega)$ values, the refractive index $n(\omega)$, absorption coefficients $\alpha(\omega)$, energy loss function $L(\omega)$, and reflectivity $R(\omega)$ are computed using the equations reported elsewhere.^{12,56–58}

The electronic properties of crystalline materials are majorly characterized by $\varepsilon_2(\omega)$, which is linked to the photon absorption phenomenon.⁵⁹ The electronic band structures showed direct bandgaps for the K_2NiP_2 ternary compound and are consistent with

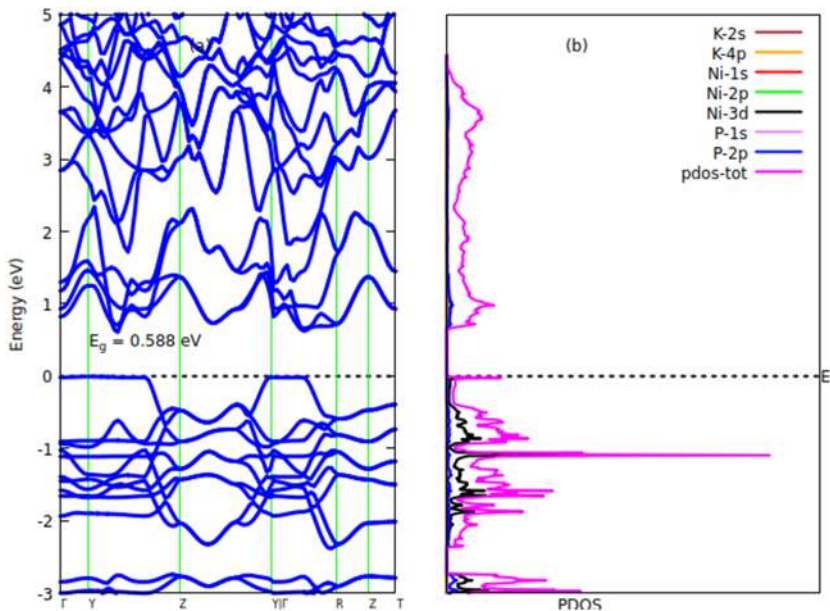


FIG. 4. Calculated (a) band structure and (b) projected density of states of K_2NiP_2 ternary compound using the GGA-PBEsol approximation.

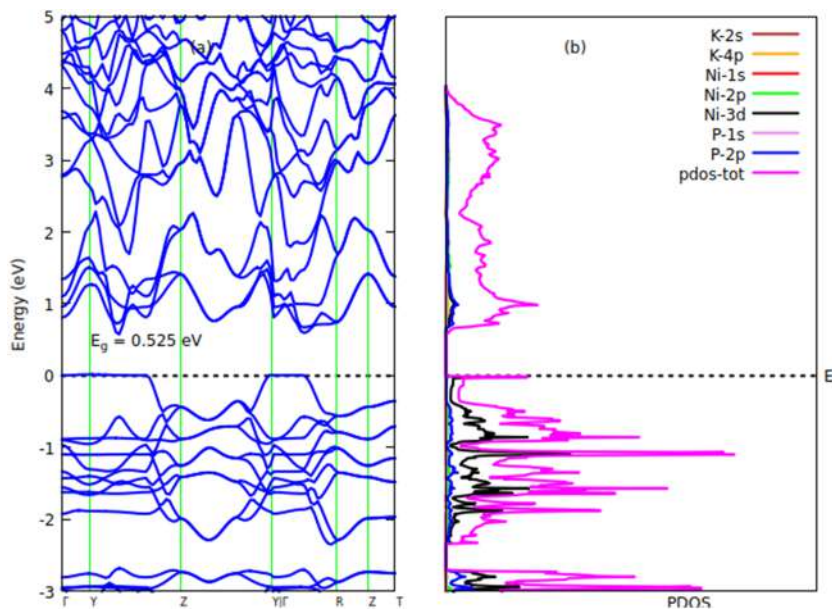


FIG. 5. Calculated (a) band structure and (b) projected density of states of K_2NiP_2 ternary compound using the LDA approximation.

the optical absorption onsets in $\epsilon_2(\omega)$ spectra. Peaks in $\epsilon_2(\omega)$ spectra result from electronic transitions from the valence to the conduction bands. The $\epsilon_2(\omega)$ curves attain their maximum at 5.071, 4.966, and 4.835 eV for the GGA-PBE, GGA-PBEsol, and LDA approximations, respectively. Thereafter, the $\epsilon_2(\omega)$ spectra decreased with an increase in energy. The fundamental component of the $\epsilon_1(\omega)$ plot is $\epsilon_1(\text{Energy} = 0)$, also denoted as the static point.⁵⁹ The obtained static values in Fig. 6(b) are 7.249, 7.426, and 7.653 for the GGA-PBE, GGA-PBEsol, and LDA approximations, respectively. The square root of these static values gives the refractive indices of the K_2NiP_2 ternary compound. From Energy = 0, the $\epsilon_1(\omega)$ plot attained its maximum at 1.219 eV for all three approximations. The photon transmission continued until the $\epsilon_1(\omega)$ plot became negative at energy regions 6.250–11.675 eV. At this point, the incident photon radiations are presumed to be fully attenuated,⁶⁰ and the K_2NiP_2 ternary compound asserts a metallic behavior.⁶¹

The refractive indices of K_2NiP_2 ternary compounds are shown in Fig. 6(c). The obtained values are about 2.683, 2.717, and 2.763 for the GGA-PBE, GGA-PBEsol, and LDA approximations, respectively. The material under investigation is, therefore, suitable for applications where large refractive indices are fundamentals. The refractive indices are high in infrared (IR) and visible regions and then decrease in the higher energy regions. Also, the refractive

indices are inversely related to the bandgaps of the compound under investigation. The refractive indices are observed to be increasing as the bandgaps decrease. The absorption coefficient spectra show the depth of light of specific photon energy that can penetrate the material before being fully absorbed.⁶² As shown in Fig. 6(d), the absorption coefficient spectra grow sharply close to 2.560 eV. The major peaks appear at 6.884–8.503 eV, and after this energy region, the spectra undergo drastic decrement. Also, the optical absorption coefficient spectra of the K_2NiP_2 ternary compound cover the ultraviolet-visible (UV-Vis) regions in the range of 2.560–13.862 eV, which imply that it can be utilized for photovoltaic applications.

TABLE IV. Voigt–Reuss–Hill Approximations of bulk modulus B (GPa), Young's modulus E (GPa), Shear modulus G (GPa), Pugh's ratio B/G, and Poisson's ratio, ν .

Compound	B	E	G	B/G	ν
PBE	24.91	35.57	14.11	1.77	0.26
PBEsol	20.22	32.63	13.27	1.52	0.23
LDA	16.54	29.56	12.32	1.34	0.20

TABLE III. Computed elastic constants, C_{ij} (GPa), of K_2NiP_2 ternary compound.

Compound	C_{11}	C_{12}	C_{13}	C_{22}	C_{23}	C_{33}	C_{44}	C_{55}	C_{66}
PBE	48.36	15.37	6.26	33.60	23.70	53.30	21.91	9.75	15.61
PBEsol	43.37	10.19	2.16	27.67	19.80	48.49	21.61	8.98	13.60
LDA	40.84	6.75	−1.65	22.96	16.30	44.52	20.79	8.05	11.30

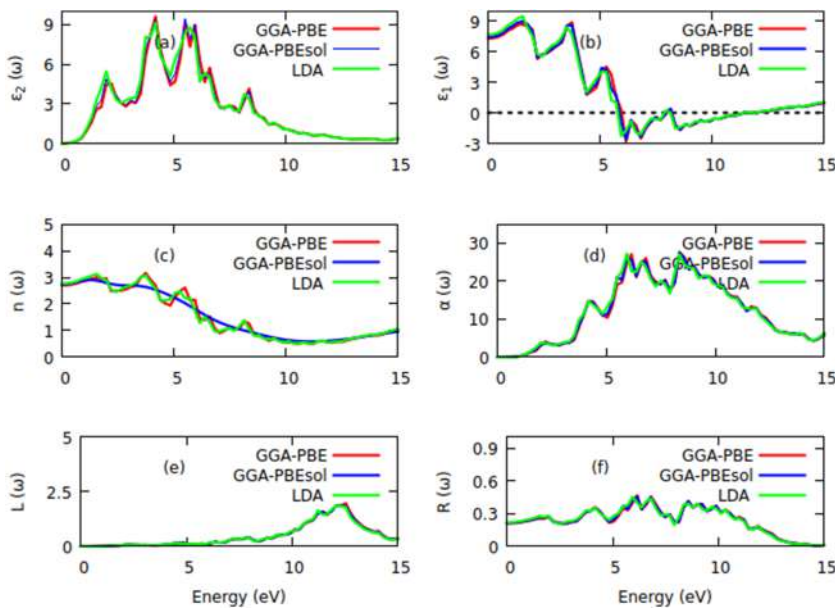


FIG. 6. (a)–(f) The imaginary dielectric function, real dielectric function, refractive index, absorption coefficient, energy loss function, and reflectivity of K_2NiP_2 ternary compound using the GGA-PBE, GGA-PBEsol, and LDA approximations.

The energy loss function describes the energy loss by an electron passing through the material.⁵⁸ There was no significant absorption in the lower energy regions as depicted in the loss spectrum. The major absorption peaks occurred at 12.015 eV. Reflectivity is an optical property that describes the optical response of the surfaces of materials.⁵⁸ From Fig. 6(f), it is observed that the reflectivity curve of the K_2NiP_2 ternary compound reaches its maximum value at the energy region 5.762–9.308 eV and then decreases beyond this region. These findings are consistent with the ones reported for materials with similar stoichiometry.²⁶

E. Conclusion

The structural, electronic, elastic, mechanical, and optical properties of the K_2NiP_2 ternary compound have been investigated using density functional theory formalism as implemented in the quantum espresso code. The calculations have been performed using the GGA-PBE, GGA-PBEsol, and LDA approximations. The ground-state lattice constants of 7.657, 7.511, and 7.372 Å have been obtained using the GGA-PBE, GGA-PBEsol, and LDA approximations, respectively. Direct bandgaps of 0.630, 0.588, and 0.525 eV have been observed using the GGA-PBE, GGA-PBEsol, and LDA approximations respectively. The valence bands are majorly formed by Ni-3d and P-2p states with little contribution from the other states, while the conduction bands are majorly formed by P-2p states with a small contribution from the other states. The compound under investigation is mechanically stable, ductile, and ionic. The computed optical properties have shown that the studied compound has refractive indices of 2.683, 2.717, and 2.763 for the GGA-PBE, GGA-PBEsol, and LDA approximations, respectively. Additionally, the studied compound has been found to have absorption coefficient spectra covering the UV–Vis part of the electromagnetic spectrum in the energy region 2.560–13.862 eV. We can, therefore, conclude that the estimated direct bandgaps, high refractive indices, high absorption coefficients, and wide energy coverage of the absorption

coefficient spectra, mainly in the UV–Vis regions, make the K_2NiP_2 ternary compound suitable for chemical coating and photovoltaic applications.

ACKNOWLEDGMENTS

The authors acknowledge the Partnership for Skills in Applied Sciences, Engineering and Technology (PASET)—Regional Scholarship Innovation Fund (RSIF) for the Funding opportunity; ISP is thanked for providing seed funding for computing resources through the KEN02 grant and also gratefully thanked the Center for High-Performance Computing, CHPC, Cape Town, RSA, for computing resources.

AUTHOR DECLARATIONS

Conflict of Interest

The authors have no conflicts to disclose.

Author Contributions

Mwende Mbilo: Conceptualization (equal); Data curation (equal); Formal analysis (equal); Investigation (equal); Methodology (equal); Validation (equal); Visualization (equal); Writing—original draft (equal); Writing—review & editing (equal). **Robinson Musembi:** Conceptualization (equal); Data curation (equal); Formal analysis (equal); Funding acquisition (equal); Investigation (equal); Methodology (equal); Project administration (equal); Resources (equal); Software (equal); Supervision (equal); Validation (equal); Visualization (equal); Writing—original draft (equal); Writing—review & editing (equal).

DATA AVAILABILITY

The data that support the findings of this study are available from the corresponding author upon reasonable request.

REFERENCES

- ¹P. A. Iles, *IRE Trans. Mil. Electron.* **MIL-6**, 5 (1962).
- ²H. Brooks, *Adv. Electron. Electron Phys.* **7**, 85 (1955).
- ³R. S. Caldwell and H. Y. Fan, *Phys. Rev.* **114**, 664 (1959).
- ⁴A. D. Dhass, Y. Prakash, and K. C. Ramya, *Mater. Today: Proc.* **33**, 732 (2020).
- ⁵H. C. Chou, A. Rohatgi, N. M. Jokerst, S. Kamra, S. R. Stock, S. L. Lowrie, R. K. Ahrenkiel, and D. H. Levi, *Mater. Chem. Phys.* **43**, 178 (1996).
- ⁶P. Giannozzi, S. de Gironcoli, P. Pavone, and S. Baroni, *Phys. Rev. B* **43**, 7231 (1991).
- ⁷I. Vurgaftman, J. R. Meyer, and L. R. Ram-Mohan, *J. Appl. Phys.* **89**, 5815 (2001).
- ⁸T. F. Kuech, *Prog. Cryst. Growth Charact. Mater.* **62**, 352 (2016).
- ⁹N. Si Ziani, H. Bouhani-Benziene, M. Baira, A. Belfedal, and M. Sahnoun, *Renewable Energy for Smart and Sustainable Cities ICAIRES 2018. Lecture in Networks and Systems* (Springer, Switzerland, 2019), Vol. 62, pp. 552–559.
- ¹⁰A. Gani, O. Cheref, M. Ghezali, M. Rabah, A. H. Reshak, Y. Djaballah, H. Righi, D. Rached, and A. Belasri, *Chin. J. Phys.* **64**, 174 (2020).
- ¹¹H. Singh, M. Singh, and M. K. Kashyap, *AIP Conf. Proc.* **1349**, 1069 (2011).
- ¹²S. Sahin, Y. O. Ciftci, K. Colakoglu, and N. Korozlu, *J. Alloys Compd.* **529**, 1 (2012).
- ¹³J. Zhang, G. Hodes, Z. Jin, and S. (Frank) Liu, *Angew. Chem., Int. Ed.* **58**, 15596 (2019).
- ¹⁴S. Lathwal, A. Gaur, K. Khan, S. K. Goyal, A. Soni, and J. Sahariya, *IOP Conf. Ser.: Mater. Sci. Eng.* **1225**, 012020 (2022).
- ¹⁵M. S. Yaseen, G. Murtaza, and R. M. Arif Khalil, *Opt. Quantum Electron.* **51**, 367 (2019).
- ¹⁶I. Ghazal, H. Absike, A. Rachadi, and H. Ez-Zahraouy, *Optik* **260**, 169077 (2022).
- ¹⁷P. Ranjan, P. Kumar, T. Chakraborty, M. Sharma, and S. Sharma, *Mater. Chem. Phys.* **241**, 122346 (2020).
- ¹⁸S. R. Thahirunnisa, I. B. Shameem Banu, M. Mohamed Sheik Sirajuddeen, and I. N. Lone, *Comput. Condens. Matter* **29**, e00601 (2021).
- ¹⁹F. Parvin and S. H. Naqib, *Results Phys.* **21**, 103848 (2021).
- ²⁰M. M. Mridha and S. H. Naqib, *Phys. Scr.* **95**, 105809 (2020).
- ²¹U. Kumar, S. Nayak, S. Chakrabarty, S. Bhattacharjee, and S.-C. Lee, *J. Mater. Sci.* **55**, 9448 (2020).
- ²²S. R. Thahirunnisa and I. B. Shameem Banu, *Appl. Phys. A* **124**, 801 (2018).
- ²³N. Megag, M. Ibrir, M. Hadjab, S. Berri, and N. Bouarissa, *Comput. Condens. Matter* **28**, e00577 (2021).
- ²⁴P. Ranjan and T. Chakraborty, *Mater. Sci. Semicond. Process.* **127**, 105745 (2021).
- ²⁵S. Fahad, G. Murtaza, T. Ouahrani, R. Khenata, M. Yousaf, S. B. Omran, and S. Mohammad, *J. Alloys Compd.* **646**, 211 (2015).
- ²⁶M. Irfan, S. Azam, and A. Iqbal, *Int. J. Energy Res.* **45**, 2980 (2021).
- ²⁷M. Somer, M. Hartweg, K. Peters, and H. G. von Schnering, *Z. Kristallogr. - Cryst. Mater.* **193**, 291 (1990).
- ²⁸P. Hohenberg and W. Kohn, *Phys. Rev.* **136**, B864 (1964).
- ²⁹W. Kohn and L. J. Sham, *Phys. Rev.* **140**, A1133 (1965).
- ³⁰P. E. Blöchl, *Phys. Rev. B* **50**, 17953 (1994).
- ³¹P. Giannozzi, S. Baroni, N. Bonini, M. Calandra, R. Car, C. Cavazzoni, D. Ceresoli, G. L. Chiarotti, M. Cococcioni, I. Dabo, A. Dal Corso, S. de Gironcoli, S. Fabris, G. Fratesi, R. Gebauer, U. Gerstmann, C. Gougoussis, A. Kokalj, M. Lazzeri, L. Martin-Samos, N. Marzari, F. Mauri, R. Mazzarello, S. Paolini, A. Pasquarello, L. Paulatto, C. Sbraccia, S. Scandolo, G. Sclauzero, A. P. Seitsonen, A. Smogunov, P. Umari, and R. M. Wentzcovitch, *J. Phys.: Condens. Matter* **21**, 395502 (2009).
- ³²Y. Wang and J. P. Perdew, *Phys. Rev. B* **44**, 13298 (1991).
- ³³J. P. Perdew and Y. Wang, *Phys. Rev. B* **98**, 079904 (2018).
- ³⁴J. P. Perdew, K. Burke, and M. Ernzerhof, *Generalized Gradient Approximation Made Simple* (Springer, Switzerland, 1996).
- ³⁵P. Ziesche, S. Kurth, and J. P. Perdew, *Comput. Mater. Sci.* **11**, 122 (1998).
- ³⁶N. Argaman and G. Makov, *Am. J. Phys.* **68**, 69 (2000).
- ³⁷R. G. Parr, *Annu. Rev. Phys. Chem.* **34**, 631 (1983).
- ³⁸S. Kotochigova, Z. H. Levine, E. L. Shirley, M. D. Stiles, and C. W. Clark, *Phys. Rev. A* **55**, 191 (1997).
- ³⁹S. P. Ong, S. Cholia, A. Jain, M. Brafman, D. Gunter, G. Ceder, and K. A. Persson, *Comput. Mater. Sci.* **97**, 209 (2015).
- ⁴⁰G. Hautier, C. Fischer, V. Ehrlicher, A. Jain, and G. Ceder, *Inorg. Chem.* **50**, 656 (2011).
- ⁴¹S. P. Ong, W. D. Richards, A. Jain, G. Hautier, M. Kocher, S. Cholia, D. Gunter, V. L. Chevrier, K. A. Persson, and G. Ceder, *Comput. Mater. Sci.* **68**, 314 (2013).
- ⁴²G. Prandini, A. Marrazzo, I. E. Castelli, N. Mounet, and N. Marzari, *npj Comput. Mater.* **4**, 72 (2018).
- ⁴³T. Katsura and Y. Tange, *Minerals* **9**, 745 (2019).
- ⁴⁴K. M. Wong, *Jpn. J. Appl. Phys.* **48**, 085002 (2009).
- ⁴⁵K. M. Wong, *Results Phys.* **7**, 1308 (2017).
- ⁴⁶G. S. Manyali, R. Warmbier, and A. Quandt, *Comput. Mater. Sci.* **79**, 710 (2013).
- ⁴⁷M. Mbilo, G. S. Manyali, and R. J. Musembi, *Comput. Condens. Matter* **32**, e00726 (2022).
- ⁴⁸S. Bağcı, S. Duman, H. M. Tütüncü, and G. P. Srivastava, *Phys. Rev. B* **79**, 125326 (2009).
- ⁴⁹F. Mouhat and F.-X. Coudert, *Phys. Rev. B* **90**, 224104 (2014).
- ⁵⁰P.-L. Yan, J.-M. Zhang, B. Zhou, and K.-W. Xu, *J. Phys. D: Appl. Phys.* **49**, 255002 (2016).
- ⁵¹S. Ozdemir Kart and T. Cagin, *J. Alloys Compd.* **508**, 177 (2010).
- ⁵²S. Tariq, A. Ahmed, S. Saad, and S. Tariq, *AIP Adv.* **5**, 077111 (2015).
- ⁵³V. Kumar and B. P. Singh, *Indian J. Phys.* **92**, 29 (2018).
- ⁵⁴A. Srivastava, P. Sarkar, S. K. Tripathy, T. R. Lenka, P. S. Menon, F. Lin, and A. G. Aberle, *Sol. Energy* **209**, 206 (2020).
- ⁵⁵R. Bhattacharjee and S. Chattopadhyaya, *Mater. Chem. Phys.* **199**, 295 (2017).
- ⁵⁶G. Nazir, S. Tariq, A. Afaq, Q. Mahmood, S. Saad, A. Mahmood, and S. Tariq, *Acta Phys. Pol., A* **133**, 105 (2018).
- ⁵⁷F. Okbi, S. Lakel, S. Benramache, and K. Almi, *Semiconductors* **54**, 58 (2020).
- ⁵⁸M. S. Yaseen, J. Sun, H. Fang, G. Murtaza, and D. S. Sholl, *Solid State Sci.* **111**, 106508 (2021).
- ⁵⁹S. Azam, M. Irfan, Z. Abbas, M. Rani, T. Saleem, A. Younus, N. Akhtar, B. Liaqat, M. Shabbir, and A. G. Al-Sehemi, *Mater. Res. Express* **6**, 116314 (2019).
- ⁶⁰G. Murtaza and I. Ahmad, *Physica B* **406**, 3222 (2011).
- ⁶¹G. Murtaza, I. Ahmad, B. Amin, A. Afaq, M. Maqbool, J. Maqssod, I. Khan, and M. Zahid, *Opt. Mater.* **33**, 553 (2011).
- ⁶²S. Khalid, Y. Ma, X. Sun, G. Zhou, H. Wu, G. Lu, Z. Yang, J. Khan, R. Khenata, and A. Bouhemadou, *J. Mater. Res. Technol.* **9**, 413 (2020).